

Low-Temperature, Sol-Gel-Synthesized, Silver-Doped Titanium Oxide Coatings to Improve Ultraviolet-Blocking Properties for Cotton Fabrics

Nurhan Onar,¹ M. Faruk Ebeoglugil,² Isıl Kayatekin,² Erdal Celik²

¹Department of Textile Engineering, Faculty of Engineering, Dokuz Eylul University, Bornova, Izmir 35040, Turkey

²Department of Metallurgical and Materials Engineering, Faculty of Engineering, Dokuz Eylul University, Buca, Izmir 35160, Turkey

Received 10 December 2006; accepted 20 March 2007

DOI 10.1002/app.26495

Published online 26 June 2007 in Wiley InterScience (www.interscience.wiley.com).

ABSTRACT: A new finishing process for cotton fabrics was developed that includes the treatment of cotton fabrics by a pad-dry-cure method with different amounts of Ag-doped, Ti-based transparent solutions prepared with a sol-gel method. Within this framework, transparent solutions were prepared with solutions of Ag- and Ti-based precursors, isopropyl alcohol, and glacial acetic acid. Then, cotton fabrics were padded with these solutions. After these processes, the padded fabrics were dried at 80°C for 30 min in air, and the coated fabrics were cured at 150°C for 5 min to produce Ag-doped TiO₂ films on the fabrics. The turbidity, pH, wettability, and rheological properties of the prepared solutions were measured. The thermal, structural, and microstructural properties of the coatings were extensively characterized with differential thermal analysis/thermogravimetry, Fourier transform infrared, X-ray diffraction, and scanning

electron microscopy/energy-dispersive spectroscopy. The thicknesses of the films were estimated with a refractometer and a spectrophotometer. In addition, the add-on values, wash fastness, ultraviolet protection, lightness, and contact angles of the coated fabrics were determined. The treatment of the fabrics with a 30 atom % Ag doped, Ti-based solution imparted to the fabrics a good ultraviolet-protection factor rating of 15+, which was an increase of 10+ in comparison with the ultraviolet-protection factor of the untreated fabric (5+). The produced fabrics were also water-resistant. Hence, this method produced multifunctional fabrics that were water-resistant and ultraviolet-protective. © 2007 Wiley Periodicals, Inc. *J Appl Polym Sci* 106: 514–525, 2007

Key words: coatings; fibers; nanolayers; polycondensation; thin films

INTRODUCTION

The efficiencies of ultraviolet (UV)-protective finishing processes depend on the weave design, color, and previous treatments of fabrics. The desired washing fastness of textiles cannot be achieved by conventional UV-protective finishing processes, and the use of chemicals in high concentrations has been necessary. On the other hand, it is necessary to impart UV-protective properties to fine cotton fabrics worn in hot weather in the summer to protect our bodies from various skin problems, such as sunburn, premature skin aging, allergies, and even skin cancer, that are caused by exposure to excessive UV radiation.

Known UV-protective finishing processes are performed through the application to fabrics of various UV absorbers of the phenol type (e.g., *o*-hydroxybenzophenone, *o*-hydroxyphenylbenzotriazole, and *o*-hydroxyphenyltriazine derivatives) and the non-

phenolic type (e.g., okzanilite and 2-cyanoacrylate).¹ In addition, optical whitening agents and various dye-stuffs as UV absorbers are used. For this aim, the use of optical whitening agents based on stilbene and triazine is explained in refs. 2 and 3. However, the efficiency of these agents should be improved because the agents have the disadvantages of low formulability and low solubility. Patents WO 97/44422 and WO 96/03486 report the use of phenylbenzotriazole, dibenzoylmethane, *p*-aminobenzoic ester, cinnamic ester, salicylic ester (not containing nitrogen), 2-hydroxybenzophenone, phenylbenzimidazole, and 2-cyano-3,3-diphenylacrylic ester agents for protecting dyed textile materials against fading from UV rays.^{4,5} In these cases, the efficiency of the agents should be improved because the agents have some disadvantages, including insufficient UV stability.

TiO₂ has drawn attention because of its nontoxicity, its chemical stability at high temperatures, and the durability of its good UV-protective power under UV-exposure conditions. For that reason, the penetration into fibers of pigments such as TiO₂ and ZnO is another fabrication technique for UV-protective fabrics. Notably, the penetration of agents into polyamide,

Correspondence to: N. Onar (nurhan.onar@deu.edu.tr).

polyester, and polyacrylonitrile fibers is useful for achieving UV-protective properties for the fibers. For this purpose, polyester fibers that have UV-protective properties with washing fastness have been produced by the addition of powder particles of TiO₂ to fiber drawing solutions.⁶

Hombitec S 100, manufactured by Sachtleben, Inc. (Duisburg, Germany), with the objective of UV protection, consists of nanoparticles in a TiO₂-based powder. A TiO₂ particle stabilized with antimony is placed in the nucleus of these particles. The particle sides are surrounded with a layer containing Al₂O₃ and ZrO₂, and radicals are possibly caught. There is also a membrane formed from organic compounds that provides good wettability and good dispersibility properties for particles in the outermost layer. Polyesters with three different qualities have been produced, and these particles have been added to the drawing solutions of polyester fibers.⁷

Nakatani and Otsuka⁸ determined that solid detergents and, in particular, soaps containing 0.1–15% ZnO have good UV-absorbing properties. Edwards et al.⁹ reported that inorganic particles can be applied to textiles with the assistance of an organic binder during the laundering of cloth and that the treated fabrics acquire UV-protective properties. As demonstrated in the research of Heidenfelder and Detering,¹⁰ UV-absorber agents together and TiO₂ and ZnO pigments separately can be mixed into washing detergents and applied to textiles. UV-protective properties are imparted to textiles with these agents. Furthermore, the use of both organic and inorganic UV-absorber chemical agents creates a synergistic effect. Additionally, Soane and Offord¹¹ patented the idea that TiO₂, ZnO, SiO₂, and Fe₂O₃ particles with 3-(triethoxysilyl) propylsuccinic anhydride, *N*-(3-triethoxysilylpropyl) gluconamide, or both with a polymer containing epoxide or cross-bonding agents alone based on poly(ethylene imine) can be bonded to cotton fabric surfaces. The UV transmission values of the fabrics are reduced by the particles bonded to the fabric.

Crystalline TiO₂ has several applications, such as photocatalysts, photovoltaics, UV absorbers, gas sensors, and electrochromic display devices, because of its photocatalytic activity and optical properties. In particular, TiO₂ exists in three crystal forms (anatase, rutile, and brookite) and has an amorphous structure. Of these crystalline forms, the anatase phase of TiO₂ has the highest photocatalytic activity. Thus, interest in the photocatalytic activity of anatase has recently grown. Photocatalytic activity means the decomposition of organic and inorganic pollutants under UV light. There is a good relationship between the absorption intensity of UV radiation and the activity of the catalysts. The stronger the UV absorption intensity is of the crystal TiO₂, the higher the photocatalytic activity is.¹² Nevertheless, because

TABLE I
Rated UPFs According to Australian/New Zealand Standard 4399 : 1996

Rated UPF	Mean UVA (effective UV transmission)	Rating
15–24	6.7–4.2	Good
25–30	4.1–2.6	Very good
>40	<2.5	Excellent

^a The data was taken from ref. 19.

it is necessary to use high temperatures of 500–550°C to produce these films, the production of photocatalytic TiO₂ films should be deposited at low temperatures on plastics and textiles that cannot withstand high-temperature treatments.

Daoud and Xin¹³ produced TiO₂ thin films on cotton fabrics by a sol-gel process at low temperatures (e.g., 150°C), and they determined that the ultraviolet-protection factor (UPF) rating of the fabrics increased from 10+ to 50+, which corresponded to excellent protection (see Table I). It is necessary to obtain good wash fastness for coated textiles, especially because textiles are exposed many more times to washing during wearing. Hence, cotton fabrics to which the process has been applied have been found to be withstand 20¹³ or even 55¹⁴ home launderings in the literature.¹⁵ Therefore, up to now, mostly TiO₂ particles have been bonded to fabrics with organic binders or through mixing in detergents. Through the development of sol-gel technologies in the last years, it has been determined that TiO₂ films can be coated onto fabrics with Ti-based solutions without an organic binder, and their UV-protective properties are improved. However, the UV-protective properties of Ag-doped, TiO₂-coated fabrics have not been investigated yet. It is possible to produce higher UV-protective properties for coated fabrics with Ag-doped, Ti-based solutions together with higher washing fastness properties and the use of lower amounts of chemical agents.

This study was devoted to the research of 10, 18, and 30% Ag doped TiO₂ films prepared on cotton fabrics from solutions of titanium isopropoxide, AgNO₃, isopropyl alcohol (C₃H₈O), and glacial acetic acid (CH₃COOH) with a sol-gel technique without an organic binder to improve their UV-protective and washing-fastness properties. To this end, the turbidity, pH measurements, wettability, and rheological properties of the prepared Ti- and Ag-based solutions were determined. To define the chemical structure and reaction type of the intermediate-temperature products and to use a suitable process regime, differential thermal analysis/thermogravimetry (DTA-TG) and Fourier transform infrared (FTIR) instruments were used in the film production. A structural analysis of the produced films was performed with multipurpose X-ray diffraction (XRD),

and the surface morphology was investigated with scanning electron microscopy (SEM)/energy-dispersive spectroscopy. The thickness of the produced films on glass was investigated with refractometer and spectrophotometer devices to estimate the real thickness on the fabric. In addition, the add-on values, wash fastness, UPF, lightness, and contact angles of the coated fabrics were determined.

EXPERIMENTAL

Nanosol preparation

To reach the aim of the study, nanosol solutions were prepared as the flow chart in Figure 1 shows. Ag-doped TiO₂ films were synthesized with solutions prepared as follows. The Ag- and Ti-based precursors were weighed out in a fume hood. C₃H₈O (Riedel, Steinheim, Germany; 99%) as a solvent and CH₃COOH (Aldrich, Steinheim, Germany; 97%) as a chelating agent were mixed in a powder form of the AgNO₃ precursor chemical agent (Aldrich; 97%). After this solution was stirred at room temperature for 30 min in air, the liquid form of titanium isopropoxide [Ti(OC₃H₇)₄; Alfa Easer, Karlsruhe, Germany] was added dropwise to this solution. The obtained solution was stirred for 3 h to obtain a transparent solution. The Ag contents in the solutions were $x = 10, 18,$ and 30 atom %, where x was calculated as $x = [\text{Ag}/(\text{Ti} + \text{Ag})] \times 100$. The stability of the process was set by control of the hydrolysis and condensation reactions such that while the solutions were being dried, the solvent was lost or the temperature was elevated.

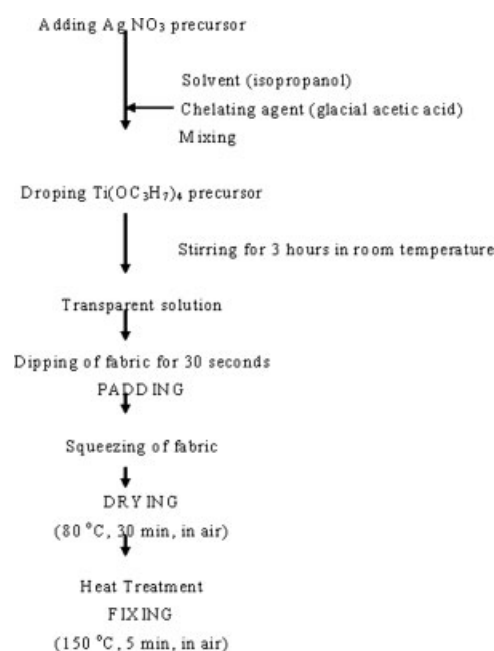


Figure 1 Flow chart for the sol-gel process.

Solution characterization

To determine the solution characteristics that affected the thin-film structure, the turbidity, pH values, wettability, and rheological properties of the prepared solutions were measured. The turbidity properties of the solutions were measured to use standard solutions for the coating process with a Scientifica TB 1 Velp turbidimeter (Usmate, Milano, Italy) according to the ISO 7027 nephelometric method. The sample was placed in a vessel with dimensions with diameter of 25 mm and height of 50 mm. Formazin is recognized throughout the world as a primary standard. A formazin solution was used to calibrate the turbidity. The measurements were taken in the range of 0–1000 nephelometric turbidity units. After the preparation of the transparent solutions, the pH values of the solutions were measured to determine their acidic and basic characteristics with a standard pH meter (WTW Inolab, Weilheim, Germany). The pH values of the transparent solutions varied from 1 to 2. The wettability properties of the solutions were determined by the measurement of their contact angles with a KSV CAM 100 contact-angle machine. Additionally, the rheological behavior of the solutions, including the viscosity, was determined with a CVO 100 digital rheometer (Bohlin Instrument, Worcestershire, UK).

Coating process

Cotton fabrics (10 cm × 10 cm), which were desized, scoured, and bleached, (weft density = 20 yarn/cm, warp density = 24 yarn/cm, weight density = 138 g/m²) were dipped at 25°C for 30 s into the solutions, and then the padded fabrics were squeezed twice with a rapid fulard (model P-A1, Labortex, Taipei, Taiwan) for 87% pickup at a nip pressure of 2.8 kg/cm². We repeated this procedure from one layer to six layers. Then, the padded fabrics were dried at 80°C for 30 min to drive off the solvent (C₃H₈O) in a preheated Nüve KD400 oven (Nüve Inc., Ankara, Turkey) in an air atmosphere. Finally, the dried fabrics were cured at 150°C for 5 min with a preheated rapid steamer ((without steam; model H-TS-3, Labortex; see Fig. 1 for details).

Film characterization

The thermal behaviors of the Ag- and Ti-based powders, which were dried at 300°C for 4 h in air, were evaluated to determine the decomposition and phase formation at a heating rate of 10°C/min in the temperature range of 25–700°C under an oxygen atmosphere with a DTA-TG machine (DTG-60H, Shimadzu, Kyoto, Japan). Al₂O₃ powder was used as a reference material. The enthalpies of solvent

removal and combustion were obtained with TA 60WS software from Shimadzu (60AH). This software derived the enthalpies through the calculation of the total area under each peak with respect to the base line from the starting temperature to the ending temperature. FTIR (PerkinElmer Inc., Beaconsfields UK) absorption spectra of the 18 atom % Ag doped samples were measured only over the range of 4000–400 cm^{-1} at room temperature after reactions in the temperature range of 25–500°C for 60 min in air. After the powders were prepared at these temperatures, they were mixed with potassium bromide (KBr). All five samples were characterized with FTIR. The transmittance/wave number and absorbance/wave number curves were obtained. According to the results, depending on the temperature, the variation of an organic component's concentration could be determined by the Fluka library supplied by PerkinElmer.

The phase analysis of the Ag-doped TiO_2 films coated on cotton fabrics was performed with a Rigaku D Max-2200/PC X-ray diffractometer (Rigaku Corp., Tokyo, Japan) at 40 kV and 20 mA with monochromatic $\text{Cu K}\alpha$ irradiation (wavelength = 0.15418 nm) in both the θ – 2θ mode and the 2θ scan mode with a scan speed of 8°/min. Thin-film XRD geometry in which the incident angle was fixed at 1° was used to collect data from only thin films. (The surface topographies of the Ag-doped TiO_2 films were examined with a JEOL JJM 6060 scanning electron microscope attached to an energy-dispersive spectroscopy apparatus.) (JEOL Ltd., Tokyo, Japan).

Before the deposition of the cotton fabrics, Ag-doped TiO_2 films with a single layer on the glass substrates were made with the sol–gel drop-coating method. The coated glass substrates were dried at 180°C for 30 min and then sintered at 500°C for 4 h with a tube oven.¹⁶ The film thickness of the produced Ag-doped TiO_2 films was evaluated with a refractometer and a spectrophotometer. The refractive indices of the thin films were measured in the visible region with an Abbe high-accuracy refractometer (Bioiberica, Barcelona, Spain) at room temperature. The refractive indices were used to determine the film thickness with a Jasco V-530 ultraviolet–visible spectrophotometer (Jasco Inc., Tokyo, Japan) in the range of 190–800 nm as follows:

$$d = \frac{1}{2\sqrt{n^2 - \sin^2 \phi}} \times \frac{\lambda_1 \times \lambda_2}{\lambda_1 - \lambda_2} \times \frac{p}{1000}$$

$$= \frac{1}{2\sqrt{n^2 - \sin^2 \phi}} \times \frac{p}{r_1 - r_2} \times 10^4 [\mu\text{m}] \quad (1)$$

where d is the film thickness, n is the refractive index measured by a refractometer, λ_1 and λ_2 are the peak wavelengths (both peaks or valleys; nm), r_1

TABLE II
Refractive Index and Thickness Values of Films Coated on Glass Substrates

Property	10 atom % Ag doped TiO_2 film	18 atom % Ag doped TiO_2 film	30 atom % Ag doped TiO_2 film
Refractive index	1.3169	1.3220	1.3115
Thickness (nm)	749	309	306

and r_2 are the numbers of the peak wavelengths (cm^{-1}), and p is the number of interference waves between λ_1 and λ_2 .

The refractive index and thickness values of the films on the glass substrates are listed in Table II. Hence, the thicknesses of the Ag-doped TiO_2 films on cotton fabrics were roughly estimated before textile application.

Textile characterization

To better understand the textile properties of the coated fabrics, the add-on values, wash fastness, UPF, lightness, and contact-angle characteristics of the coated fabrics were investigated. The add-on values of the coated fabric were calculated as follows:

$$W_{\text{add-on}}(\%) = \frac{W_2 - W_1}{W_1} \times 100 \quad (2)$$

where W_1 is the dry weight of the untreated fabric, W_2 is the dry weight of the treated fabric, and $W_{\text{add-on}}$ is the add-on value of the untreated fabric. The dry weights of the fabrics were determined. The treated and untreated fabrics were conditioned under a standard atmosphere of $20 \pm 2^\circ\text{C}$ and $65 \pm 2\%$ relative humidity for 24 h before the weighing.¹⁷ The wash fastnesses of the samples were determined according to BS EN ISO Standard 105-C06-A1S (without balls) with a Linitest Plus apparatus (Atlas, Gelnhausen, Germany).¹⁸ The washing processes were performed 1 time and 10 times. The microstructures of the coated fabrics were studied with images of the samples taken before and after washing with a JEOL JSM-6060 scanning electron microscope operating at 3 kV with 2000× magnification. The UV-protective characteristics of the coated fabrics were determined according to Australian/New Zealand Standard 4399 : 1996 with a Camspec M350 ultraviolet–visible spectrophotometer (Camspec Ltd., Stockport, England).¹⁹ The lightness values of the prepared fabrics were determined with a Minolta 3600d spectrophotometer (Konica Minolta Inc., Osaka, Japan). The contact angles of the fabrics were determined with a KSV CAM 100 instrument to determine the water-repellent properties of the fabrics.

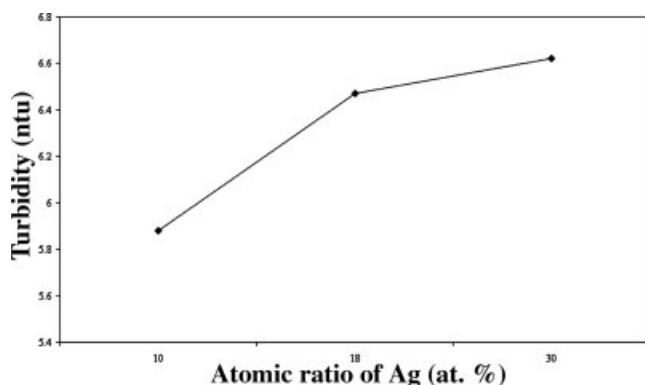


Figure 2 Turbidity values of the prepared solutions.

RESULTS AND DISCUSSION

Solution characteristics

Turbidimetric measurements were used to reveal the complete dissolution of the powder-based precursors in the solutions. Figure 2 presents the turbidity values of the prepared transparent solutions. Their turbidity values were in the range of 6–6.8 nephelometric turbidity units, indicating that the powder-based chemical precursors had completely dissolved in the solutions. With the addition of the AgNO_3 powder to the solutions, no significant change in the turbidity was observed. The same behavior was found for all the solutions in the presence of AgNO_3 . Figure 2 shows that the turbidity increased slightly as the Ag content increased, and this suggests the evolution of larger aggregates because the thermodynamic conditions of the system became gradually poorer as the charge neutralization point between the polyelectrolyte and the oppositely charged ions was approached. This is one of the general characteristics of transparent solutions. It is evidence that transparent solutions were formed in this case. The turbidity values are important in the formation of very thin films on fabrics from Ag-doped TiO_2 solutions after the synthesis process.

A characteristic feature of many sol-gel solutions is the dependence of the viscosity on the shear rate or test time. Figure 3 depicts the measured viscosity for Ag- and Ti-based solutions in the presence of various amounts of Ag as a function of the test time. These viscosity curves illustrate the viscosities as a function of increasing test time. However, when the subsequent decline in the test time was probed (not shown here), no significant hysteresis effects were detected; that is, the up-ramp curve and down-ramp curve practically coincided. The decrease in the viscosity with the increasing test time could be attributed to the breakup of association complexes or network junctions; that is, the rate of disruption of

the complexes exceeded the rate at which associations were reformed. It was determined that the viscosity of the solutions with different contents of Ag was approximately equal to 2 mPa s. The viscosity values of every three solutions were similar to the values for diluted solutions, suggesting that this was a key factor in controlling the film thickness. Because the thin films were formed from diluted solutions, these results were reasonable for sol-gel processing. In our case, Ag-based TiO_2 films were obtained with low-viscosity diluted solutions. Moreover, the fact that there was practically no change in the viscosity upon the addition of Ag to the solutions showed that the network was not significantly reinforced. In this respect, it is interesting to note that parallel results could be found in the turbidity study, in which smaller differences were observed among the solutions. Depending on the test time, a small decrease in the viscosity in solutions probably signals fragmentation of the network as strong association complexes are formed.²⁰ However, to find a strong decrease in the viscosity in solutions or a gel point as a result of this, the test time should be prolonged.

In the measurement of the contact angles of the solutions, the main aim was to obtain information about the wettability of the solutions. As we demonstrated in detail for sol-gel coatings elsewhere²¹ and briefly summarize here, the wettability properties of solutions give important clues for further processes in the sol-gel technique concerning how to produce crack-free, pinhole-free, continuous, and textured films before film fabrication is begun. The properties of spreading liquids on substrates present the film quality. If the contact angle is 0, the liquid is said to be a spreading liquid, and the solid will be covered with a liquid film. When the contact angle is 0, crack-free films are produced because of very thin gels on the substrate. However, if the contact angle is greater than 0, the solution liquid does not spread on the substrate. In that case, thick gel films form on

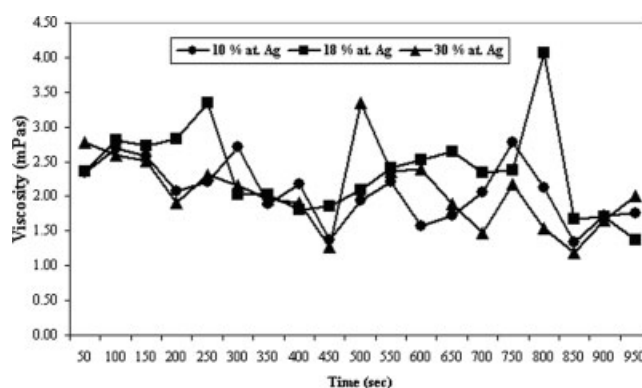


Figure 3 Viscosity values of the prepared Ag-doped, Ti-based transparent solutions.

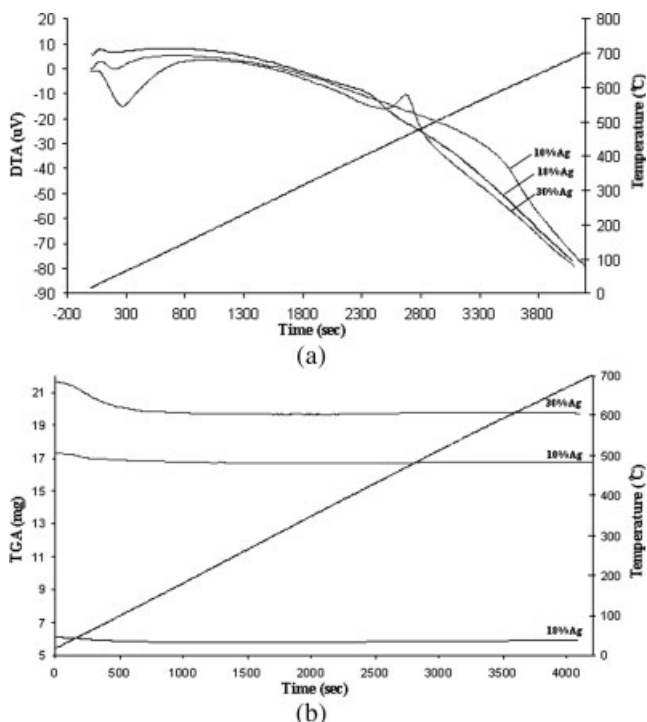


Figure 4 (a) DTA and (b) TG curves of powders obtained from 10, 18, and 30 atom % Ag doped, Ti-based solutions after they were dried at 300°C for 4 h in air.

the surface of the substrate, and thus cracking occurs. In these experiments, the contact angles could not be measured because of the spreading of solutions on glass in times shorter than 20 s. The obtained results showed that the contact angles of the solutions were close to zero. On the basis of these values, it was concluded that the wettability of the prepared solutions was fairly high. It was proved that the deposition of Ag-doped TiO₂ films that were continuous, homogeneous, and crack-free depended on the wettability properties with a very low contact angle.

Film characteristics

DTA–TG analysis

Figure 4 illustrates a DTA–TG analysis of 10, 18, and 30 atom % Ag doped, Ti-based powders dried at 300°C for 4 h in air. Similarly, Sen et al.²² observed that three or four phenomena take place from room temperature to 650°C. In this study, similar results were found for Ag-doped, Ti-based powders. As indicated in the DTA curves of the Ag-doped, Ti-based powders, endothermic and exothermic reactions occurred at temperatures between 25 and 650°C. The first thermal phenomenon occurred between 68 and 107°C because of solvent removal. When we specifically investigated 10, 18, and 30 atom % Ag doped, Ti-based powders, the minimum peak temperatures corresponding to the evaporation of the solvent were 93, 68,

and 90°C, respectively, which were in good agreement with our previous studies.^{23–25} The formed enthalpies of 10, 18, and 30 atom % Ag doped TiO₂ xerogels during solvent removal were determined to be 30, 691, 2, and 227 J/g, respectively. The second phenomenon was the combustion of OR groups at temperatures between 150 and 350°C. The large and broad exothermic peaks were determined in this temperature range to be due to the decomposition of organic substances and the oxidation of some organic materials in Ag-doped TiO₂ xerogels. At this stage, combustion likely occurred with the fracture of C–O–Ag and C–O–Ti and the formation of Ag–O–Ag and Ti–O–Ti with weak bonding. On the other hand, the thermal effect in these temperature ranges was assigned to the burn-out of organic residue from the complex decomposition. It is believed that the evaporation of NO₃[−] entrapped in the xerogels, coming from the AgNO₃ precursor, occurred as well as the combustion of organic materials. The third stage was the formation of ceramic oxides between 350 and 475°C, which was in good agreement with the temperatures mentioned in the literature.^{22–25} In the last stage, an exothermic peak was found around 500°C because of anatase-to-rutile phase transformation. According to the thermophysical data of Chao et al.,²⁶ the heat is completely sufficient to warm the anatase grains from 490 to 750°C because of anatase-to-rutile phase transformation. This effect was not clearly observed for a powder based on 10 atom % Ag doped, Ti-based powder. In an 18 atom % Ag doped, Ti-based sample, a small exothermic peak was observed at 516°C due to the phase transformation. As for a 30 atom % Ag doped, Ti-based xerogel sample, a larger exothermic peak was determined at 493°C. It was deduced that the phase transformation formed at lower temperatures once the Ag content was increased in TiO₂. The formed enthalpies of 30 atom % Ag doped TiO₂ xerogels during oxidation were found to be 63 J/g. The temperatures higher than the phase transformation point were obtained locally, and the phase transformation could be greatly facilitated if the TiO₂ powder could effectively absorb the heat warming the anatase grains.²⁶

The TG curves for the 10, 18, and 30 atom % Ag doped, Ti-based xerogel powders showed weight losses of 3.00, 3.72, and 8.87% for temperatures ranging from 25 to 650°C. In this range of the thermal treatment, the weight decrease was due to solvent removal and combustion of carbon-based materials. As can be seen in the TG curves, the largest weight lost occurred during the combustion of carbon-based materials. The slope of the TG curve quickly decreased when the carbon-based materials were

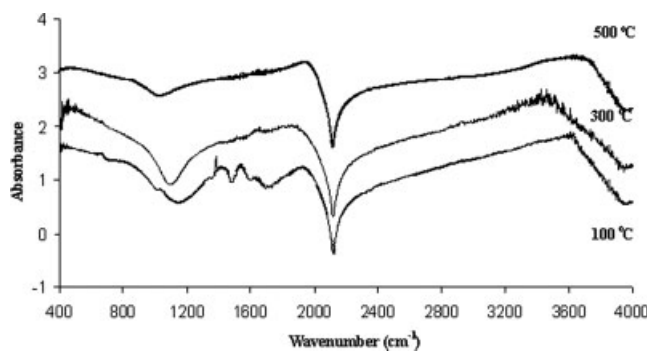


Figure 5 FTIR absorbance spectra of the prepared Ag- and Ti-based powders at different temperatures for 60 min in air.

burnt out. The variations in the enthalpies and weight losses occurred because the amounts of the xerogels used in the DTA–TG experiments differed. The amounts influenced only the enthalpies and weight losses of the materials. There was no effect on the maximum peak temperatures of combustion and oxidation because they were specific properties of the materials. As can be obviously seen in these results, the temperatures of combustion and oxidation depended on the material type, which was different.

FTIR analysis

Figure 5 shows the FTIR absorbance spectra of the prepared Ag- and Ti-based powders dried at three different temperatures (100, 300, and 500°C) for 60 min in air. The FTIR data are in accordance with the DTA–TG results. The band seen at approximately 1600 cm^{-1} was due to C=O arising from bridging-type metal–acetate bonding (M–OCOO–M). The spectra of the samples heat-treated at 100 and 300°C were quite similar. However, the OH band shifted slightly toward lower frequencies. When the heat-treatment temperature increased from 100 to 500°C, the frequencies of the O–H, C=O and M–OCOO–M bands decreased and progressively disappeared around 500°C. Therefore, around the transition temperature ($\sim 500^\circ\text{C}$), the changes were very fast, and above 450°C, no signals of O–H, C=O, and M–OCOO–M bands were found. To illustrate, the spectrum of the Ag-doped TiO_2 precursor film annealed at 500°C shows an absence of absorption bands corresponding to organics and hydroxyls, indicating the complete removal of organics and hydroxyls. The common features that appear below 600 cm^{-1} correspond to the stretching vibrations of Ag=O and Ti=O and also to the contributions of Ag–O and Ti–O bonds. In the spectrum of 500°C, the band at $\approx 450 \text{ cm}^{-1}$ can be assigned to the vibration of Ag_2O and

TiO_2 bands appearing at high temperatures.²⁷ The intensities of the bands increased with increasing temperature because of oxide formation. Likewise, the oxide content could be monitored as a function of the heat-treatment temperature changing from 25 to 500°C. The oxide formation progressively appeared with an increasing heat-treatment temperature.

Structural analysis

Figure 6 shows XRD patterns of the coated fabrics with Ag-doped TiO_2 containing 10, 18, and 30 atom % Ag. The anatase peaks for every treated fabric were observed at 16, 23, and 25°. Nevertheless, the rutile phase was not determined on account of the curing process of the treated fabrics at low temperatures (e.g., 150°C). This is evidence that anatase TiO_2 forms on cotton fabrics at low temperatures with the sol–gel method. For Ag-doped TiO_2 , the phase transformation occurs at low temperatures. As discussed in ref. 26, a pure TiO_2 film does not form at low temperatures. However, the anatase TiO_2 phase occurs when Ag is doped into TiO_2 . In addition, with Ag in the TiO_2 films, a broad peak is particularly determined to be centered at about 16°, and this indicates its amorphous character. It can also be stated that the deposition temperature increases; it is possible for high crystallinity of the TiO_2 phase to be formed, the peaks becoming sharper and highly intense. Because of a high redox potential for Ag^+ ions, by heat and TiO_2 photocatalytic reduction, the Ag^+ ions spreading on the surface anatase grains are gradually reduced into Ag^0 . For charge compensation, oxygen vacancies occur:

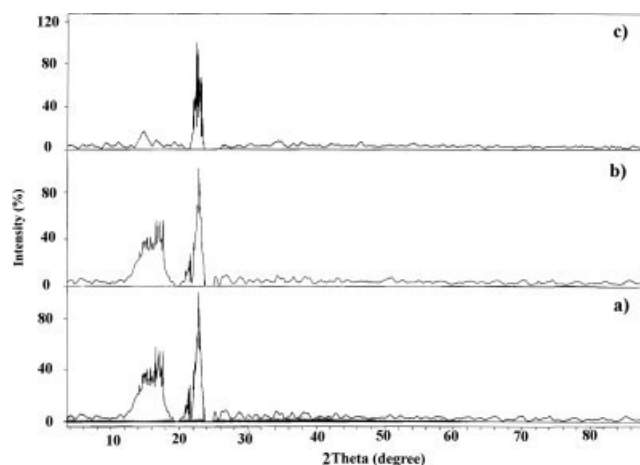
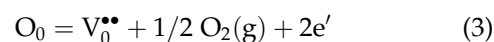


Figure 6 XRD patterns of (a) 30, (b) 18, and (c) 10 atom % Ag doped, TiO_2 -coated fabrics.

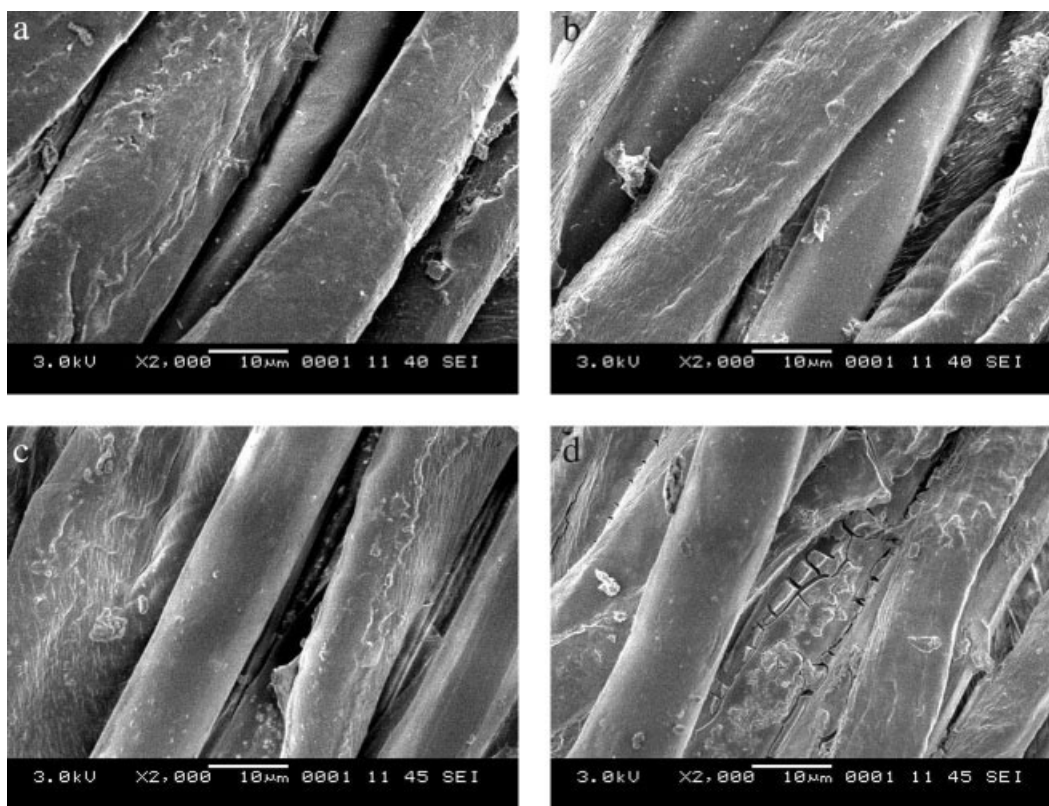


Figure 7 SEM images of (a) untreated fabrics and (b–d) fabrics treated with 10, 18, and 30 atom % Ag doped, Ti-based solutions before washing, respectively.

The concentration of oxygen vacancies at the surface of the TiO_2 grain increases, and this facilitates the bond rupture and ionic movement necessary for the formation of the rutile phase. The anatase-to-rutile phase transformation is then accelerated. Although the concentration of anion vacancies at the surface of the films may further increase with the Ag concentration, the phase transformation will not be enhanced so strongly. That suggests that the Ag dopant probably promotes the phase transformation in those TiO_2 structures in other ways. Because the specific surface area of the TiO_2 films markedly decreases, the phenomenon is probably caused by enhanced absorption of heat produced by the oxidation of organic groups and the decomposition of nitrate contained in the TiO_2 gel films during the calcination process.²⁶

Microstructural properties

Figures 7 and 8 present SEM images of untreated fabrics and fabrics treated with 10 atom % Ag doped, Ti-based solutions, 18 atom % Ag doped, Ti-based solutions, and 30 atom % Ag doped, Ti-based solutions before washing and after washing one time. According to the SEM images of the coated

fabrics with 10 and 18 atom % Ag doped TiO_2 films, the fiber surfaces were smoother than that of the untreated fabric, and as a result, the fiber surface could be coated homogeneously and smoothly with the solutions. However, it was observed from SEM images of the fabric coated with a 30 atom % Ag doped TiO_2 film that cracks formed on the fiber surface and the micrometer-order particles on the fiber surface occurred as coating islands. After washing, the coating islands peeled off from the fiber surface. It was determined that every three fabrics doped with different amounts of Ag after washing had smoother surfaces. The mean thickness of the fibers was determined to be $15\ \mu\text{m}$ with SEM. The increasing fiber thickness of the coatings was not determined, so the fiber thickness had variations in the fabric.

The film thicknesses of the coated fabrics were estimated with an optical technique. Table II shows the refractive indices and film thicknesses. The thicknesses of 10, 18, and 30 atom % Ag doped TiO_2 films were measured to be 749, 309, and 306 nm, respectively, with an optical method after layer deposition. The thicknesses of the films could be modified and the roughness could be improved by appropriate changes in the preparation conditions of the solutions and the deposition procedure.

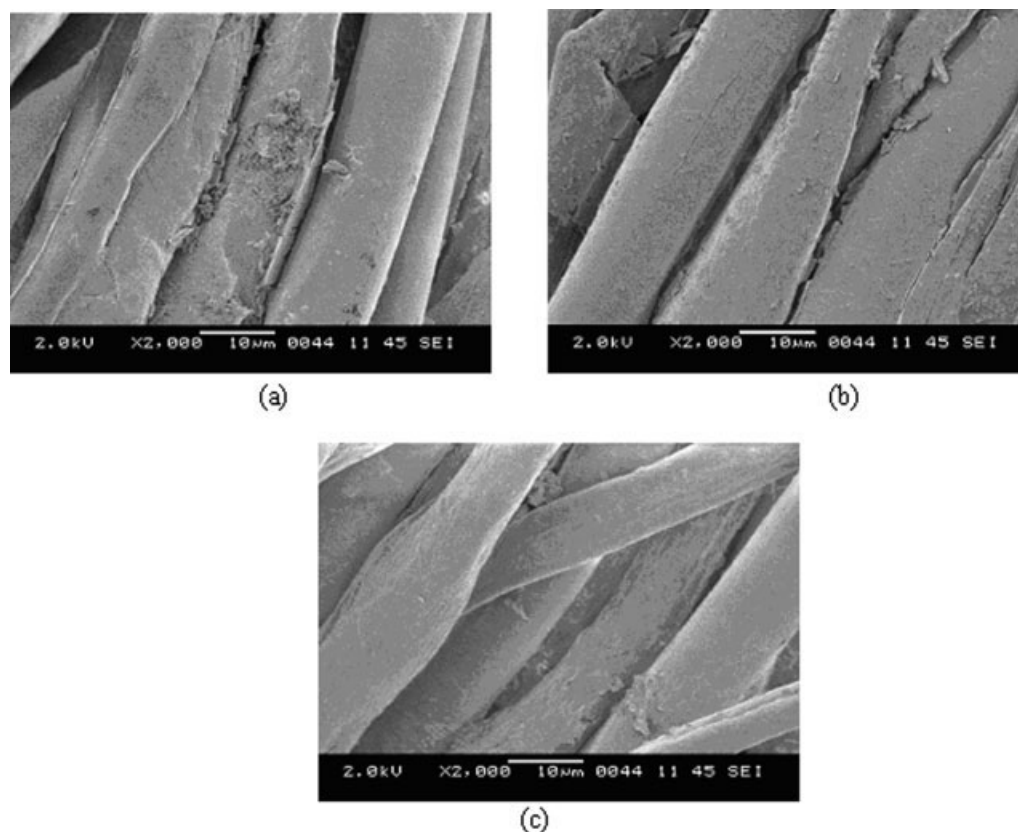


Figure 8 SEM images of the fabrics treated with (a) 10, (b) 18, and (c) 30 atom % Ag doped, Ti-based solutions after one washing.

Textile characteristics

Add-on value of the treated fabrics

Because materials with a high density and thus a high degree of coverage generally have a high UPF, as discussed in detail later, the add-on values of the fabrics will gain importance in this respect. The add-on values of the treated fabrics are shown in Figure 9. The add-on values of the treated fabrics increased when the atomic ratio of Ag in the films increased.

UV-protective characteristics of the treated fabrics

All untreated and treated textiles were examined for their protective properties by the method given in Australian/New Zealand Standard 4399 : 1996. To determine the UPF of the textile materials at a particular wavelength in the UV range, the transmittance was measured at different wavelengths in the range of 290–400 nm. The UV transmittance was determined by the comparison of the intensity at each wavelength through the untreated and treated fabric textile samples, as demonstrated elsewhere.²⁸

The UPF has been proposed as a parameter for the UV protection of fabrics. As with sunscreens,

this protection factor mainly indicates the degree of protection against UV. We have attempted to determine whether a fabric with a high UPF value could offer adequate protection in the UV-light range. The results vary according to the different materials of the untreated and treated fabrics. The UV-protective characteristics of the fabrics are systematically presented in Table III. It was determined that the fabric treated with a 30 atom % Ag doped, Ti-based solution had a 15+ UPF rating, which was increased by

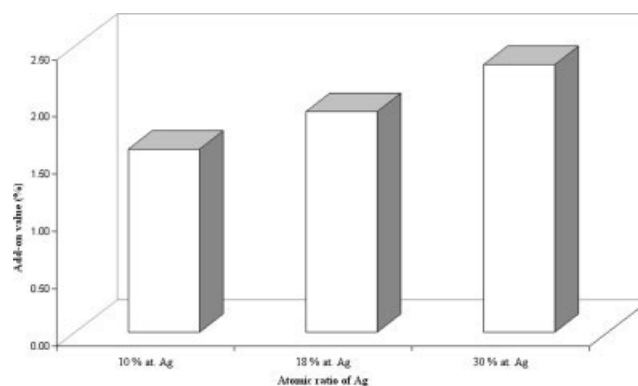


Figure 9 Add-on values of the treated fabrics.

TABLE III
Rated UPFs of Untreated Fabric and Fabrics Treated 1 Time and 6 Times Before and After Washing 1 Time and 10 Times

UV protection		Blank fabric	1A-1 ^a	2A-1 ^b	3A-1 ^c	1A ^a	2A ^b	3A ^c
Treatment 1 time after washing 1 time	Rated UPF	5	10	10	15	10	10	10
	Mean UVA (315–400 nm; %)	17.2	12.3	9.8	7.2	11.6	9.3	10.4
	Mean UVB (290–315 nm; %)	12.5	7.5	6.8	4.6	6.7	6.2	7.1
Treatment 6 times after washing 1 time	Rated UPF	5	10	10	15	10	10	15
	Mean UVA (315–400 nm; %)	17.2	10.3	11.1	8.4	9.69	8.7	7.2
	Mean UVB (290–315 nm; %)	12.5	6.9	7.4	5.8	6.0	5.9	5.2
Treatment 6 times after washing 10 times	Rated UPF	5	10	10	15	15	15	20
	Mean UVA (315–400 nm; %)	17.2	10.3	11.1	8.4	7.5	7.6	6.1
	Mean UVB (290–315 nm; %)	12.5	6.9	7.4	5.8	4.9	4.8	3.7

^a Coated fabric with 10 atom % Ag doped titania before and after washing, respectively.

^b Coated fabric with 18 atom % Ag doped titania before and after washing, respectively.

^c Coated fabric with 30 atom % Ag doped titania before and after washing, respectively.

10 in comparison with that of the untreated fabric (5+), and the rating corresponded to a good protection factor according to the relevant standard, as indicated in Table I.

The fabrics treated with 10 and 18 atom % Ag doped Ti had a 10+ UPF rating, which corresponded to an insufficient protective rating (Table III). The UPF rating of the fabrics treated with 10 and 18 atom % Ag doped, Ti-based solutions did not change after one washing, whereas the UPF rating of the fabric treated with a 30 atom % Ag doped, Ti-based solution decreased by 5+ after one washing. It was determined that the coating with less Ag-doped TiO₂ solution did not contribute to the UV-protective properties of cotton fabrics, and the coating with much more Ag-doped TiO₂ solution improved the UV-protective properties of the fabrics, but there was no effect on the wash fastness. We suggest that silver should be physically embedded into fabric

and the physically embedded silver could be removed after washing.

The UPF ratings of the fabrics treated with solutions six times were determined before and after washing. The treatment of these solutions six times increased the add-on value of the fabric to 12%. The degree of protection of the fabrics treated six times in the UV range was the same as that of the once treated fabrics before washing in the same UV range, as presented in Table III. The UPF ratings of all treated fabrics did not change after one washing. Silver should be permanently bonded to the fabric with the solution treatment performed six times, and the UV-protective properties of the fabrics with the wash fastness should increase. In research parallel to our work, Standford et al.²⁹ reported that the UV-protective properties of cloth would increase with washing and wearing. The UPF ratings of the treated fabrics increased after 10 washings in agreement with this study. Their UPF ratings increased with washing, so the withdrawn fabric after multiple washings regained a much denser form.

Furthermore, it was considered that the silicate forms contained in the composition of an ECE phosphate

TABLE IV
Composition of the ECE Reference Detergent

Composition	Mass fraction (%)
Linear sodium alkyl benzene sulfonate (mean length of alkane chain C = 11.5)	8.0 ± 0.02
Ethoxylated tallow alcohol (14 EO)	2.9 ± 0.02
Sodium soap (C ₁₂ –C ₁₆ chain length: 13–26%, C ₁₈ –C ₂₂ chain length: 74–87%)	3.5 ± 0.02
Sodium tripolyphosphate	43.7 ± 0.02
Sodium silicate (SiO ₂ /Na ₂ O = 3.3/1)	7.5 ± 0.02
Magnesium silicate	1.9 ± 0.02
Carboxymethylcellulose	1.2 ± 0.02
Ethylenediaminetetraacetic acid, sodium salt	0.2 ± 0.02
Sodium sulfate	21.2 ± 0.02
Water	9.9 ± 0.02
Total	100.00

^a The data were taken from ref. 18. EO, ethoxylate.

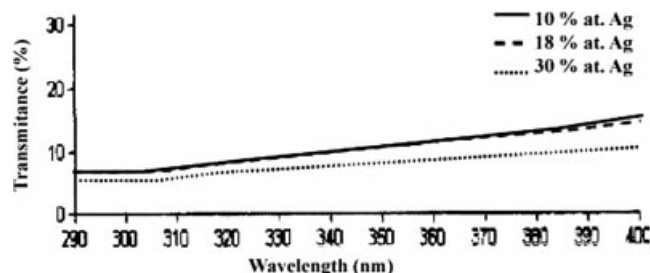


Figure 10 Spectra of the transmission of UV rays of fabrics treated six times with different atomic ratios of Ag-doped, Ti-based solutions before washing.

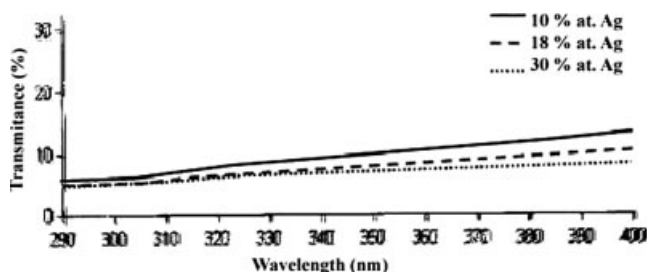


Figure 11 Spectra of the transmission of UV rays of fabrics treated six times with different atomic ratios of Ag-doped, Ti-based solutions and then washed one time.

reference detergent (B; see Table IV) according to BS EN ISO Standard 105-C06-A1S could increase the UV-protective ratings of the fabrics after multiwashing.³⁰ Therefore, the UV transmission values, related to the wavelength of the treated fabrics, decreased, whereas the applied silver amount increased, and the lowest UV transmission values were obtained after 10 washings, as graphically presented in Figures 10–12.

Lightness features

The lightness values of the treated fabrics are shown in Figure 13. Considerable variation between the photometric data and the results of the corresponding coated and uncoated fabrics was observed. It was determined that the lightness values of the fabrics decreased as a function of the Ag content in the coated fabrics. The lightness values of the treated fabrics slightly increased after washing. No variation in the lightness results could be seen because the silver salt and titanium alkoxide precursors dissolved very well in the solutions. Hence, the white fabric changed in color, from yellow to brown, after the coating process, but the physically embedded silver in the fabric with the washing of the treated fabrics could be removed, and thus the color became lighter. These results agreed with the changing UPF ratings of the treated fabrics after washing. In addition, Figure 14 shows pictures of fabrics treated six times with solutions before and after 10 washings with 10, 18, and 30 atom % Ag doped TiO₂.

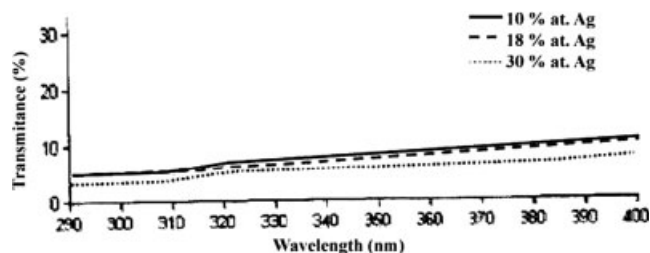


Figure 12 Spectra of the transmission of UV rays of fabrics treated six times with different atomic ratios of Ag-doped, Ti-based solutions and then washed 10 times.

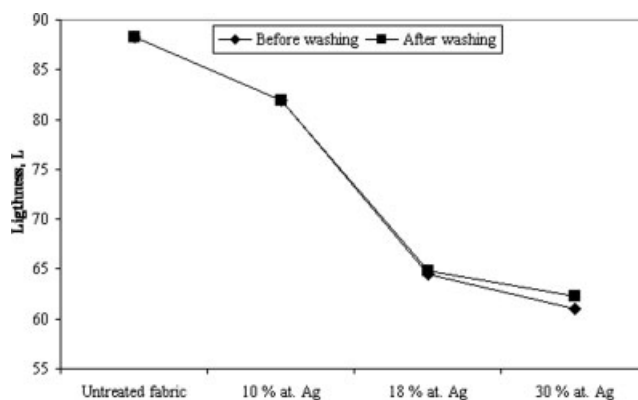


Figure 13 Lightness values of the treated fabrics.

Wettability and hydrophobic properties

To evaluate the hydrophobic properties of such coatings, the contact-angle measurements were performed first on the coated cotton fabric substrates. The contact angles of untreated and treated fabrics are shown in Table V. Figure 15 shows the contact angles of fabric treated with a 10 atom % Ag doped, Ti-based solution. The contact angles could not be measured, so the water drop at the surface of the untreated fabric spread in a time shorter than 20 s. Hence, the hydrophilicity and wettability of the untreated fabrics were high. The contact angles of the treated fabrics before and after washing were fairly high (127°). However, it was determined that the contact angle of the treated fabric with a 30 atom

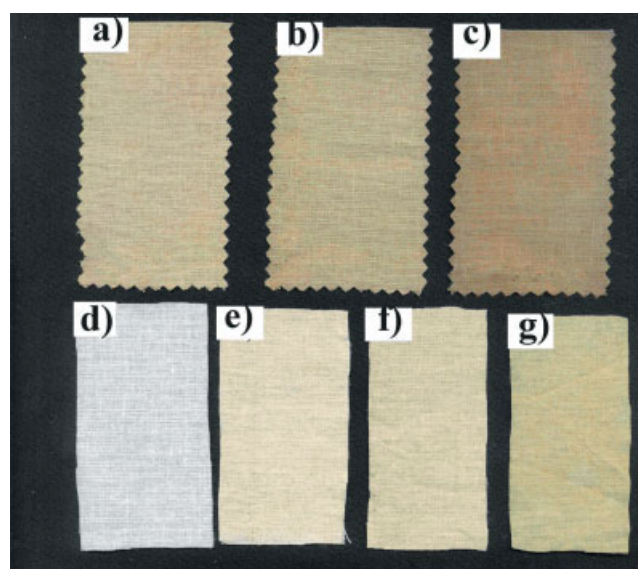


Figure 14 Fabrics treated six times with solutions before and after washing: (a) 10, (b) 18, and (c) 30 atom % Ag doped TiO₂ films on the fabric before washing; (d) untreated fabric; and (e) 10, (f) 18, and (g) 30 atom % Ag doped TiO₂ films on the fabric after washing 10 times. [Color figure can be viewed in the online issue, which is available at www.interscience.wiley.com.]

TABLE V
Contact Angles of the Untreated and Treated Fabrics

	Untreated fabric	1A-1 ^a	2A-1 ^b	3A-1 ^c	1A ^a	2A ^b	3A ^c
Contact angle	Not measurable	127°	127°	128°	131°	127°	118°

^a Coated fabric with 10 atom % Ag doped titania before and after washing, respectively.

^b Coated fabric with 18 atom % Ag doped titania before and after washing, respectively.

^c Coated fabric with 30 atom % Ag doped titania before and after washing, respectively.

% Ag-doped Ti solution showed a reduction of 10° after washing with respect to the other fabrics. However, the water resistance for the sample was still high. The results showed compliance with the changes in the lightness and UPF after washing, and as a result, the hydrophobic property of the fabric could be reduced with the removal of physically embedded silver in the fabric. On the other hand, treating cotton fabric with Ag-doped Ti solutions imparted to the fabric water resistance with wash fastness. On the basis of these results, it could be stated that coatings with suitably sized Ag-doped TiO₂ films on cotton fabrics showed increased hydrophobic properties.

CONCLUSIONS

With a newly developed UV-protective finishing process for cotton fabrics, the best results were

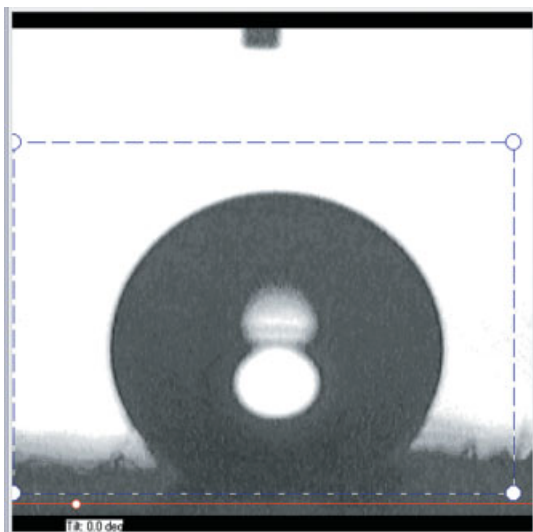


Figure 15 Contact angles of fabric treated with a 10 atom % Ag doped, Ti-based solution. [Color figure can be viewed in the online issue, which is available at www.interscience.wiley.com.]

obtained on fabrics treated six times with 30 atom % Ag doped, Ti-based solutions. The treated fabrics had UV-protective properties with washing fastness for multiple washings. Moreover, the produced fabrics were water-resistant. As a result, water-resistant and UV-protective fabrics could be produced without binding organic chemical agents by a newly developed single-step process. Hence, this method provides multifunctional fabrics. This process is applicable to industry because of its easiness and can be possibly applied to fabrics by the generally used pad-dry-cure method at textile pretreatment departments in textile companies.

References

- Holme, I. *Int Dyer* 2003, 189, 7.
- Reinehr, D.; Eckhardt, C. *Eur. Pat. EP 0682145* (1995).
- Reinehr, D.; Eckhardt, C. *Eur. Pat. EP 0728749* (1996).
- Bird, N. P.; Finch, T. D. *Int. Pat. WO 97/44422* (1997).
- Sivik, M.; Robert, S.; John, C. *Int. Pat. WO 96/03486* (1996).
- Achwal, W. B. *Colourage* 1997, 44, 31.
- Sachtleben Chemie GmbH <http://www.sachtleben.de/include> (accessed, April 4, 2006).
- Nakatani, Y.; Otsuka, S. *Jpn. Pat. JP 03/277699* (2003).
- Edwards, S. D.; Edwards, K. *Int. Pat. WO 98/42909* (1998).
- Heidenfelder, T.; Detering, J. *U.S. Pat. 2004074012* (2004).
- Soane, D. S.; Offord, D. A. *U.S. Pat. 2003013369* (2003).
- Zhang, Y.; Xiong, G.; Yao, N.; Yang, W.; Fu, X. *Catal Today* 2001, 68, 89.
- Daoud, W. A.; Xin, J. H. *J Sol-Gel Sci Technol* 2004, 29, 25.
- Xin, H.; Daoud, W. A.; Kong, Y. Y. *Text Res J* 2004, 74, 97.
- Daoud, W. A.; Xin, J. H.; Zhang, Y.-H.; Qi, K. *J Non-Cryst Solids* 2005, 351, 1486.
- Sena, S.; Mahantya, S.; Roy, S.; Heintz, O.; Bourgeois, S.; Chaumont, D. *Thin Solid Films* 2005, 474, 245.
- Sun, G.; Xu, X.; Bickett, J. R.; Williams, J. F. *Ind Eng Chem Res* 2001, 40, 1016.
- Textile Tests for Colour Fastness Part C06: Colour Fastness to Domestic and Commercial Laundering*; BSI BS EN ISO 105-C06, British Standards Institution, London, UK, 1997.
- Sun Protective Clothing—Evaluation and Classification*; Australian/New Zealand Standard 4399: Standards Australia, Homebush, Australia and Standards New Zealand, Wellington, New Zealand 1996.
- Beheshti, N.; Nguyen, G. T. M.; Kjoniksen, A.-L.; Knudsen, K. D.; Nyström, B. *Colloid Surf A* 2006, 279, 40.
- Celik, E.; Avci, E.; Hascicek, Y. *S. Mater Sci Eng B* 2004, 110, 213.
- Sen, S.; Mahantya, S.; Roy, S.; Heintz, O.; Bourgeois, S.; Chaumont, D. *Thin Solid Films* 2005, 474, 245.
- Celik, E.; Keskin, I.; Kayatekin, I.; Ak Azem, N. F.; Ozkan, E. *Mater Charact* 2007, 58, 349.
- Celik, E.; Gokcen, Z.; Ak Azem, N. F.; Tanoglu, M.; Emrullahoglu, O. F. *Mater Sci Eng B* 2006, 132, 258.
- Celik, E.; Yildiz, A. Y.; Tanoglu, M.; Ak Azem, N. F.; Toparli, M.; Emrullahoglu, O. F.; Ozdemir, I. *Mater Sci Eng B* 2006, 129, 193.
- Chao, H. E.; Yun, Y. U.; Xingfang, H. U.; Larbot, A. *J Eur Ceram Soc* 2003, 23, 1457.
- Ning, W.; Shen, H.; Liu, H. *Appl Catal* 2001, 211, 153.
- Czajkowski, W.; Paluszkiwicz, J.; Stolarski, R.; Kazmierska, M.; Grzesiak, E. *Dyes Pigments* 2006, 71, 224.
- Standford, D. G.; Georgouras, K. E.; Pailthorpe, M. T. *J Eur Acad Dermatol* 1997, 8, 12.
- Yu, M.; Gu, G.; Meng, W. D.; Qing, F. L. *Appl Surf Sci* 2007, 253, 2304.